Heliyon 10 (2024) e31495

Contents lists available at ScienceDirect

Heliyon

journal homepage: www.cell.com/heliyon

Research article

Ammonium ion removal from aqueous solutions in the presence of organic compounds, using biochar from banana leaves. Competitive isotherm models

Fernanda Pantoja [a], Sándor Beszédes [b], Tamás Gyulavári [c], Erzsébet Illés [d], Gábor Kozma [c], Zsuzsanna László [b,*]

[a] Doctoral School of Environmental Sciences, University of Szeged, H-6720, Szeged, Hungary
[b] Department of Process Engineering, University of Szeged, H-6725, Szeged, Hungary
[c] Department of Applied and Environmental Chemistry, Institute of Chemistry, University of Szeged, Rerrich Béla Sqr. 1, H-6720, Szeged, Hungary
[d] Department of Food Engineering, University of Szeged, H-6725, Szeged, Hungary

ARTICLE INFO

Keywords:
Biochar
Water treatment
Adsorption
Ammonium removal
Competitive adsorption

ABSTRACT

Background: Industrial, e.g. food industrial and domestic wastewaters contain huge amount of compounds causing eutrophication, and should be removed with high cost during wastewater treatment. However, these compounds could be utilized as fertilizers too. Biochar can remove a wide range of pollutants from water, such as ammonium, which can be found in relatively high concentration in dairy wastewaters. However, adsorption performance may be affected by the presence of other wastewater pollutants. Thus, this study aims to determine the efficiency of biochar as an adsorbent of ammonium in aqueous solutions in the presence of some selected organic compounds of typical dairy wastewaters such as bovine serum albumin (BSA), lactose, and acetic acid. Methods: The biochar was produced from banana leaves at 300 °C, modified with NaOH, and characterized by Scanning Electron Microscope – Energy Dispersive X-Ray Spectroscopy (SEM-EDX), Fourier-transform infrared spectra (FTIR) analysis, and specific surface area measurements. Batch experiments were carried out to investigate the ammonium adsorption capacity and the ion competitive adsorption mechanism. Significant Findings: Results show that the surface structure of the biochar derived from banana leaves is different from other biochars previously studied; although the specific surface area is not very considerable and despite having nitrogen within the elemental composition, the biochar studied is capable of adsorbing 2.60 mg NH_4^+/m^2, the highest ammonium removal in 2 h occurs at pH 9 and 500 mg biochar dose. Langmuir model in the monolayer phase analysis fits better for all scenarios and the maximum NH_4^+ adsorption capacity was 0.97 mg/g without organic compounds. In the multilayer adsorption phase, the isotherm model that best fits the data obtained is the Harkins-Jura model without organic compounds. The presence of organic compounds in the aqueous solution significantly impacts the adsorption of ammonium by biochar since it improves the adsorption capacity (1.132 mg/g BSA, 0.975 mg/g lactose, and 1.874 mg/g acetic acid). The Aranovich-Donohue isotherm model fitted the data obtained during ion competitive adsorption experiments well.

* Corresponding author.
E-mail addresses: fliceth@hotmail.com (F. Pantoja), beszedes@mk.u-szeged.hu (S. Beszédes), gyulavarit@chem.u-szeged.hu (T. Gyulavári), illes.erzsebet@chem.u-szeged.hu (E. Illés), kozmag@chem.u-szeged.hu (G. Kozma), zsizsu@mk.u-szeged.hu (Z. László).

https://doi.org/10.1016/j.heliyon.2024.e31495
Received 20 January 2024; Received in revised form 15 May 2024; Accepted 16 May 2024
Available online 17 May 2024

1. Introduction

Currently, the world is focusing on environmental protection and the significance of preserving natural resources for human existence and maintaining the balance of the ecosystem, according to the United Nations set various sustainable development goals [1]. There are different technologies to remove contaminants from water; among them, adsorption has advantages regarding costs and efficiency [2]. Food industrial and domestic wastewaters contain huge amount of compounds causing eutrophication, and should be removed with high cost during wastewater treatment. However, these compounds could be utilized as fertilizers too. Globally, the current valuation of waste has arisen within the framework of the circular economy concept, which aims to promote the sustainability of productive systems and reduce environmental harm [3]. Agricultural waste may be a source of cellulose and starch that can be transformed into products with additional value. Agricultural waste can also be applied as a starting material of biochar, a carbonaceous material with excellent physicochemical properties for adsorbing pollutants in wastewater [4], such as ammonium, which can be found in relatively high concentration in dairy wastewaters.

Due to the increasing demand for food caused by population growth worldwide, agricultural production is rising, generating agricultural waste from plant sources [5]. One of the crops that gained attention is the banana; this peculiar fruit is available every annual season worldwide and is mainly cultivated in Asia, Latin America, and Africa. The fact that only the cluster is consumed makes the cultivation of this fruit unusual, while most of the plant is discarded, such as the rachis, pseudostem, and its prominent leaves. It was estimated that in the year 2022, the export of this fruit reached 19.6 million tons [6].

Additionally, the development of biochar-based fertilisers has generated significant interest in the scientific community, as they are low-cost and contribute to sustainability [7], providing an excellent alternative to the increasingly more expensive commercial fertilisers [8].

Ammonium ions circulate in the environmental compartments; in some cases, it is beneficial, such as in soils where it is a nutrient for plants, and in other cases, it is a pollutant that causes adverse effects such as the eutrophication of freshwater [9]. Different physicochemical methods have been developed to remove ammonium ions from industrial or domestic wastewaters; as dairy industry dairy wastewaters may contain a high amount of ammonium ions, at ~69.96 ± 1.16 mg NH_4^+/L concentration on average, it would be an ideal source for biochar and ammonium-based fertilizer. On the other hand, this type of wastewater may also contain organic compounds from industrial processes and from the nature of feedstock specially proteins [10], which may affect the adsorption process factors such as pH and temperature, and susceptibility to lose efficiency in the presence of other elements [11].

Most of the previous investigations related to ammonium ion adsorption suggest experimentation on synthetic solutions containing exclusively ammonium ions or failing that bi-solute coadsorption and tri-solute coadsorption considering ammonium, nitrates and phosphates only. Mg–Al- modified soybean straw biochars were used for single solute adsorption of ammonium, nitrate and phosphate [12], acid modified corncob biochars with different impregnation ratio biochar/nitric acid (weight/volume) were used for exclusive ammonium adsorption [13]; optimized MgO-impregnate sugarcane harvest residue biochar with different Mg concentrations were applied in the ammonium adsorption experiments with phosphate, ammonium and humate (organic component) substance solutions, simulating the composition of swine wastewater. However, the research does not analyze the impact of organic matter on the adsorption process of other substances such as ammonium and phosphates, but rather considers humate as an adsorbate [14]. Ball-milled bamboo biochar was compared with bamboo biochar in exclusive ammonium adsorption process without any interaction with other components in the aqueous solution [15]. The use of biochar as an adsorbent for removing ammonium ions from aqueous solutions has been extensively studied in the past. Research has indicated that the capacity of biochar to adsorb ammonium is significantly influenced by its surface area and pore size [16], moreover, the cation exchange capacity (CEC) of biochar can be improved by the presence of functional groups, such as acidic and functional phenolic and carboxyl groups, which will facilitate the removal of ammonium [17], while the pyrolysis temperature affect the characteristics of the material as an adsorbent; in general, at high temperatures, ammonium adsorption decreases for all feedstocks [18]. Biochar is such a good adsorbent that it is even stated that could substitute high-priced commercial adsorbent to remove ammonium from wastewater [19].

Regarding the adsorption mechanism on biochar, isotherm modelling in binary adsorption systems, some studies use models applicable to pollutant adsorption from aqueous solutions. Examples include the extended Langmuir or Langmuir-like models in the case of dye adsorption with rice husk adsorbents [20], or the Freundlich model for monometal and multimetal adsorption conditions using sesame straw biochar [21].

Considering the aforementioned background, it is important to contemplate that dairy wastewaters have organic components whose presence can affect the removal of ammonium ions through different interactions between all elements involved in the aqueous solution. Thus, this study aims to determine the efficiency of biochar as an adsorbent of ammonium in aqueous solutions in the presence of some selected organic compounds of typical dairy wastewaters such as BSA, lactose, and acetic acid, and investigate the adsorption mechanism through mono- and multilayer adsorption models. As the novelty of the present study, we investigate this aspect, and the application of multilayer and ion competitive models for adsorption process between ammonia and organic compounds (BSA, lactose and acetic acid) which can contribute to the knowledge of biochar-based adsorbents, to the development of efficient methods, and to mapping their potential in dairy wastewater treatment and waste utilization. The objectives of the present research focus on characterizing the adsorbent material, studying the adsorption behaviour of ammonium combined with other organic compounds, establishing the interaction relationship that occurs between them and the impact on the adsorption process.

2. Materials and methods

2.1. Alkaline-modified biochar preparation

Banana leaves were collected at the Botanical Garden in Szeged city. Subsequently, leaves were cut into small pieces and washed with distilled water several times to remove impurities. Then, they were dried in an oven at 105 °C for 2 h. The dried material was stirred in a 1 M NaOH solution (1:10 w/v) for 24 h and then washed several times with distilled water until the pH of the washing solution became closest to the neutral pH. The material was sifted and dried at 105 °C for 2 h. Once the material was dry, it was subjected to pyrolysis at 300 °C for 2 h in a muffle furnace (Nabertherm, LE 2/11/R6, Germany). Finally, the biochar was ground in a ceramic mortar until reaching a particle size of 250 μm, and the resulting powder was used for the adsorption experiments.

2.2. Characterization of biochar

The characterization of biochar is conducted with the objective to get a better understanding of physical and chemical characteristics, as well as changes in biochar features as a result of production. For chemical properties of biochar, the present study focused in the electrical conductivity through measurement of zeta potential, for physical properties, the surface area and pore size were determined by means of adsorption methods (BET isotherm measurements); surface morphology and elemental composition were determined by scanning electron microscopy with energy dispersive X-ray spectroscopy (SEM–EDX) and the surface functional groups were measured by Fourier-transform infra-red spectroscopy (FT-IR).

2.2.1. Zeta potential analysis

To investigate the surface chemistry of the biochar and its possible interactions with the adsorbate, we measured the zeta potential using 10 mg of biochar in a suspension mixed in bottles containing 10 mL of 0.01 M sodium chloride (NaCl) solutions at different pH values. After mixing, the equilibrium pH of the samples was measured and adjusted. Then, the zeta potential was measured by a Zetasizer NanoZs instrument (Malvern Panalytical Ltd, UK) using electrophoretic light scattering (ELS).

2.2.2. Scanning electron microscopy (SEM-EDX) analysis

The morphology of the biochar surface and the elemental composition were analyzed with a Hitachi S-4700 Type II microscope (Hitachi, Tokyo, Japan); scanning electron microscope using 10 kV accelerating voltage.

2.2.3. Fourier-transform infrared spectroscopy (FT-IR) analysis

FT-IR studies were carried out using a Bruker Vertex 70 IR spectrometer (Bruker, Billerica, MA, USA) (16 scans/s, 4 cm^{-1} resolution) using the KBr pellet technique.

2.2.4. Methylene blue adsorption and biochar surface area estimation

The specific surface area (SSA) of biochar was estimated with the methylene blue method. The procedure and the equations used are detailed in the works of Nunes et al., 2011 and Albalasmeh et al., 2020 [22,23]. In this study, 10.0 mg of banana-derived biochar was placed in 10.0 mL of methylene blue solution at different concentrations (1, 2, 3, 4, 5, and 6 mg/L) for 24 h at room temperature. The remaining concentration of methylene blue was analyzed using a UV–Vis spectrophotometer (Agilent, Cary 60UV–Vis, Malaysia) at a wavelength of 664 nm. The SSA of banana-derived biochar was estimated according to Eq. (1):

$$SSA = \frac{q_{MB} \times N_A \times A_{MB}}{1000} \quad (1)$$

where q_{MB} is the amount of methylene blue adsorbed on the biochar (mmol/g) obtained from the monolayer adsorption isotherm using the Langmuir equation, NA is Avogadro's number (6.023×10^{23} mol^{-1}) and AMB is the area covered by one methylene blue molecule (130 $Å^2$) [23].

2.2.5. Brunauer–Emmett–Teller (BET) analysis

The European Biochar Certificate EBC (2015) and the International Biochar Initiative IBI (2015), recommend the BET method to analyze nitrogen adsorption isotherms for determining SSAs. The SSA, total pore volume and average pore size of alkali-modified biochar were measured by adsorption–desorption analysis using N_2 vapour. The samples were prepared for an average of 2 h in a vacuum at 200 °C (Quantachrome Nova 3000e instrument).

2.3. Preparation of stock solutions

Ammonium chloride salt (0.5944 g; NH_4Cl) was dissolved in 1 L of distilled water to obtain a mother solution of ammonium ions with a concentration [NH_4^+] of 200 mg/L. The concentration of organic compounds was equal to or less than the [NH_4^+] in the solutions used for the biochar adsorption experiments.

Ultrapure water with an electrical conductivity of 0.323 μS/cm was produced by an ELGA equipment; the bovine serum albumin (BSA) with 96 % protein content was manufactured by VWR International Kft. (Hungary); lactose monohydrate ($C_{12}H_{22}O_{11}·H_2O$) was

produced by Flora Vita (Hungary); and acetic acid (96 %; CH_3COOH) was manufactured by VWR Prolabo (France). Sodium hydroxide and hydrochloric acid solutions with 0.1 M concentration were used to adjust the pH of the aqueous solutions.

2.4. Sorption experiments

Adsorption experiments were conducted according to the batch method, by adding biochar samples to water solutions with different concentrations of NH_4^+. The experiments were performed at different pH (from 3 to 9) and biochar dose (from 200 to 500 mg) ranges to determine their ideal value for adsorption. In order to determine the optimal contact time at which the biochar reaches maximum ammonium adsorption, adsorbate concentration measurements were carried out at the first 5 min and then every 10 min until determining that the ideal contact time is of 2 h. Fig. 6, shows the results of the effect of pH, percentage of efficiency of adsorption at different pH, the effect of dose of biochar and the effect of the contact time in the NH_4^+ adsorption process using the alkaline modified biochar derived from banana leaves. It is important to mention that preliminary experiments were carried out at a small initial ammonium ion concentration ($[NH_4^+] = 1.5$ mg/L), ammonium concentration was determined by the indophenol method. Specifically, to obtain the isotherms, we added 500 mg of biochar to 200 mL of NH_4Cl solution with a concentration of 5, 10, 25, and 50 mg NH_4^+/L. The mixture was stirred for 2 h at 250 rpm, followed by sampling (6 mL) and filtering through 0.45 μm microporous membrane filters. The NH_4^+ concentration was measured by UV–vis spectroscopy (Agilent, Cary 60UV–Vis, Malaysia) at a wavelength of 680 nm. The indophenol method was applied for the measurements (the calibration curve in this method suggests a maximum concentration 2 mg NH_4^+/L; at higher concentrations, the dilution method was applied).

The amount of NH_4^+ adsorbed per unit mass of biochar was calculated based on Eq. (2); additionally, the NH_4^+ removal rate was calculated by Eq. (3):

$$q_e = (c_i - c_e) * \frac{V}{m} \tag{2}$$

where q_e is the amount of NH_4^+ adsorbed by biochar (mg/g) at equilibrium; c_i and c_e are the NH_4^+ concentration in the initial and equilibrium solution (mg/L), respectively; V is the volume of the aqueous solution (L), and m is the mass of biochar (g).

$$\%Removal\ NH_4^+ = \frac{c_f}{c_f - c_i} * 100 \tag{3}$$

where c_f and c_i are the final and initial NH_4^+ concentrations, respectively.

The isotherm of NH_4^+ adsorption by biochar was studied through batch adsorption experiments at room temperature using different initial NH_4^+ concentrations and a constant biochar dose (500 mg). To determine the isotherm and kinetic models that effectively describe NH_4^+ adsorption, we fitted existing mathematical models to the isotherms and kinetics data by a nonlinear method using the Solver add-in command in Microsoft Excel. The best-fitting kinetic and isotherm models were selected principally based on the value of the nonlinear correlation coefficient (R^2). The chi-square (χ^2) statistics also assisted in confirming this selection. A value of χ^2 close to zero means that the selected model fits the experimental data, while a high value of χ^2 indicates that the model is inappropriate. R^2 and χ^2 were calculated using Eqs. (4) and (5), respectively:

$$R^2 = \frac{\sum \left(q_{e,cal} - q_{e,mean}\right)^2}{\sum \left(q_{e,cal} - q_{e,mean}\right)^2 + \sum \left(q_{e,cal} - q_{e,exp}\right)^2} \tag{4}$$

$$\chi^2 = \sum \frac{\left(q_{e,exp} - q_{e,cal}\right)^2}{q_{e,cal}} \tag{5}$$

where $q_{e,exp}$ (mg/g) is the amount of NH_4^+ uptake at equilibrium obtained from Eq. (2), $q_{e,cal}$ (mg/g) is the amount of NH_4^+ uptake calculated from the model using the Solver add-in command, and $q_{e,mean}$ (mg/g) is the mean of the $q_{e,exp}$ values.

The amount of adsorbate (mg) adsorbed per unit surface area (m^2) of the adsorbent was calculated by Eq. (6):

$$q_A = q_e / SSA \tag{6}$$

2.5. NH_4^+ concentration measurements

The colourimetric indophenol blue method was applied to measure NH_4^+ concentration. For this purpose, salicylate and oxidising reagents were prepared, and the calibration curve was calculated in a range between 0 and 2 mg NH_4^+/L. The samples were measured using a UV–vis spectrophotometer (Agilent Cary 60 UV-VIS, Malaysia) at a wavelength of 680 nm. At concentrations greater than 2 mg NH_4^+/L the dilution method was applied. The Beer–Lambert law was used to determine the NH_4^+ concentration based on the calibration curve.

2.6. Competitive adsorption

The alkaline-modified banana-derived biochar was soaked in a 1 M HCl solution (1:20 w/v) for 24 h, washed several times with distilled water until the pH became neutral, and dried at 80 °C. Batch experiments were conducted at room temperature using aqueous solutions with different initial concentrations of BSA, lactose, and acetic acid (10, 30, 50, and 100 ppm in all cases). The dose of banana-derived biochar was 200 mg, and the volume of solution in each experiment was 100 mL. After 2 h of contact time, 30 mL of sample was taken and filtered through 0.45 μm microporous membrane filters for total organic carbon (TOC) measurements (Teledyne Tekmar Torch equipment). Each experiment was repeated three times. Additionally, blank experiments were carried out using distilled water. Finally, a relationship between the TOC value and concentration of each organic compound was established using the competitive Langmuir-like model; then these results were used for developing the Aranovich-Donohue isotherms model.

2.7. Adsorption models

The Solver function available in Microsoft Excel was used for fitting the non-linear isotherm models to the experimental data. The function aims to minimise the sum of the squared difference between the experimental data and the predicted data [24]. The Langmuir, Freundlich, BET, and Harkins Jura isotherm models were applied using Eqs. (7)–(10), respectively, as follows:

$$\frac{c_e}{q_e} = \frac{1}{q_{max}} c_e + \frac{1}{K \bullet q_{max}} \tag{7}$$

where c_e is the equilibrium concentration of ammonium ions (mg/L), q_e is the solid phase concentration of ammonium ions (mg/g), and q_{max} (mg/g) and K (L/mg) are empirical constants.

$$ln\, q_e = ln\, K_f + \frac{1}{n} ln\, C_e \tag{8}$$

where K_f is the Freundlich characteristic constant [(mg/g) $(L/g)^{1/n}$] and 1/n is the heterogeneity factor of sorption.

$$q_e = \frac{Q_m K_S C_e}{(1 - K_L C_e)[1 + (K_S - K_L) C_e]} \tag{9}$$

where q_e is the total amount of NH_4^+ adsorbed on the adsorbent at equilibrium (mg/g), Q_m is the amount of NH_4^+ adsorbed at the available sites on the surface of the adsorbent (i.e., monolayer) (mg/g); c_e is the NH_4^+ concentration at equilibrium (mg/L), K_S is the monolayer adsorption equilibrium constant (L/mg), and K_L is the multilayer adsorption equilibrium constant (L/mg).

$$\frac{1}{q_e^2} = \frac{B}{A} - \left(\frac{1}{A}\right) \log c_e \tag{10}$$

where A and B are constants in the Harkins–Jura model characterized by multilayer adsorption at a relatively large distance from the surface [25].

Extended Langmuir model was used for competitive adsorption between ammonium ions, biochar and organic compounds. The equation of this model is presented in Eq. (11):

$$\theta_1 = \frac{A * c_{eq1}}{1 + A * c_{eq1} + B * c_{eq2}} \tag{11}$$

where θ is the fraction of the surface covered by an adsorbed component, c_{eq} is the concentration of a component at equilibrium, and A and B are affinity constants of components 1 and 2, respectively [26].

The Aranovich–Donohue (AD) equation is an empirical method to fit multilayer adsorption isotherms. The equation is composed of two terms. The first one describes the behaviour of adsorption at the first molecular layer, and the second one describes multilayer adsorption [27]. Eq. (12) present the AD model as follows:

$$q = f(c) * \frac{1}{(1 - b_2 C)^{n2}} \tag{12}$$

The first term is the function f(c) that can be expressed using any model simulating a Type I isotherm. In the present work, this model was considered a Langmuir-like model or competitive adsorption (Eq. (11)). Eqs. (13) and (14) were used for AD models in competitive adsorption between each organic compound, biochar and NH_4^+:

$$q_{e1} = \frac{K_{L1} Q_{m1} c_{e1}}{1 + K_{L1} c_{e1} + K_{L2} c_{e2}} * \frac{1}{(1 - b_2 c_{e1})^{n2}} \tag{13}$$

$$q_{e2} = \frac{K_{L2} Q_{m2} c_{e2}}{1 + K_{L2} c_{e2} + K_{L1} c_{e1}} * \frac{1}{(1 - b_3 c_{e2})^{n3}} \tag{14}$$

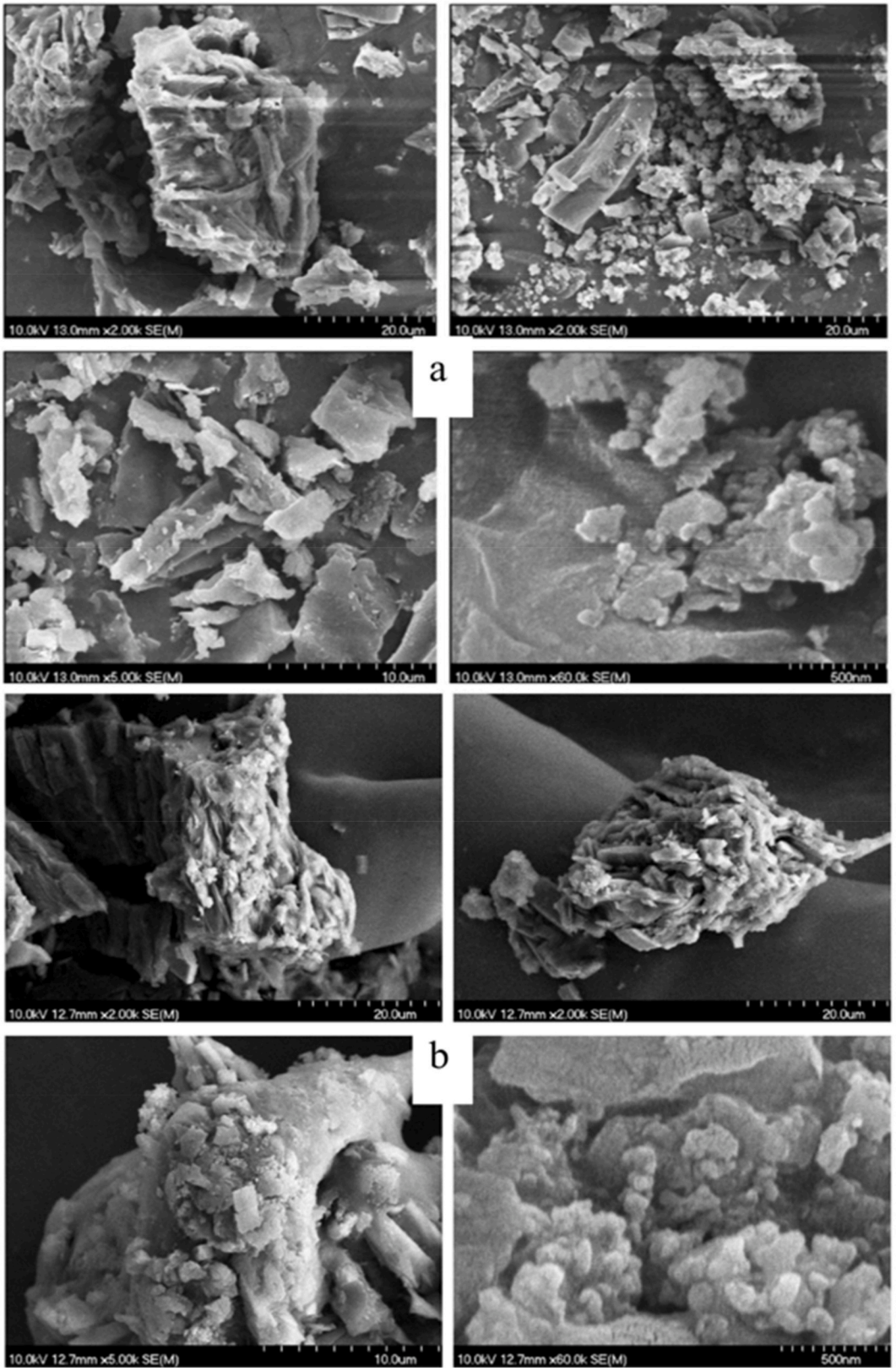

Fig. 1. Scanning electron microscope images of biochar. a) before NH_4^+ ion removal and b) after NH_4^+ ion removal.

where b_2 and n_2 are the fitting constants for NH_4^+, and b_3 and n_3 are the fitting constants for the organic compound in the AD model.

3. Results and discussion

3.1. Characterization of alkali-modified banana-derived biochar

3.1.1. SEM analysis

Surface morphology is a significant factor in adsorbent–adsorbate interactions. Fig. 1 shows the surface morphology of alkali-modified biochar in the part a) (four first pictures). The material has a rough, irregular surface. Additionally, the pore structure extends inward, which result is similar to the one presented in the paper of Cao et al. who analyzed leaf-derived biochar [28]. Similar SEM images were shown in the work of Rafique et al. for biochar produced from jujube (*Ziziphus spina-christi*) leaves [29]. In the research of Ali T et al., banana peels waste biochar produced at 350 °C shown the similar results of SEM images as the present study [30]. The part b) of Fig. 1 (last four pictures) show the surface morphology of the biochar after the ammonium ion removal, the void spaces that the surface of the biochar presented before the adsorption process are visibly smaller in the biochar after the ammonium has been adsorbed.

3.1.2. EDX analysis

The quantitative chemical analysis of the modified biochar showed that before ammonium adsorption, the biochar has Carbon 24.60 %, Nitrogen 17.32 %, Oxygen 47.23 %, Magnesium 4.17 %, Silicon 1.62 % and Calcium 4.09 %; after the adsorption process the elemental composition of biochar change in percentages detailed as follows: Carbon 24.17 %, Nitrogen 21.86 %, Oxygen 45.10 %, Magnesium 3.66 %, Silicon 3.37 % and Calcium 4.41 %. Previous researches have highlighted the importance of the elemental composition in biochars, elements such as carbon, oxygen [31], and the presence of other elements like calcium, potassium, and chlorine [32] play a significant role in determining the adsorption capacity, stability, and potential environmental applications of biochar. The presence of Nitrogen in the biochar analyzed in the present work is mainly due to the raw material from which it is derived. Furthermore, the alkali modification of biochar, alter its elemental composition and properties. For instance, introduce new elements and functional groups, impacting the surface charge, the adsorption efficiency and reactivity of biochar. Fig. 2 shows the elemental composition of modified biochar 2a) before adsorption and 2b) after the adsorption process.

3.1.3. FT-IR analysis

FT-IR analysis was carried out for the samples modified with NaOH to study the changes in functional groups (Fig. 3). The FT-IR spectra show that both samples include a variety of functional groups that may influence the NH_4^+ adsorption process. Table 1 summarizes the identified functional groups.

A broad and sharp band was observed at 3434 cm^{-1}, indicating that biochar contains OH functional groups. These groups are important in NH_4^+ adsorption because they can form coordination bonds with N atoms [34]. The bands at around 2851, 1613, 1319, and 782 cm^{-1} indicate saturated C–H, C═C or N–H, –OH, and N–H functional groups, respectively. The results obtained are comparable with some previous investigations on various biochar samples. Specifically, they are similar to the results obtained by Yang

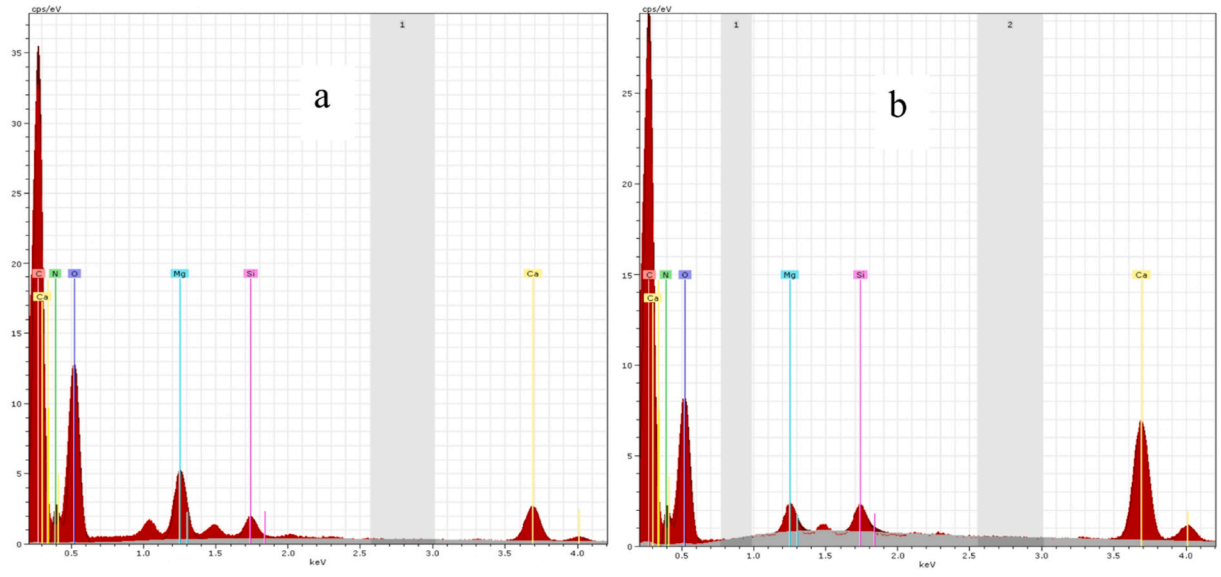

Fig. 2. a) Elemental composition of modified biochar derived from banana leaves and b) Elemental composition of modified biochar derived from banana leaves after NH_4^+ ion removal.

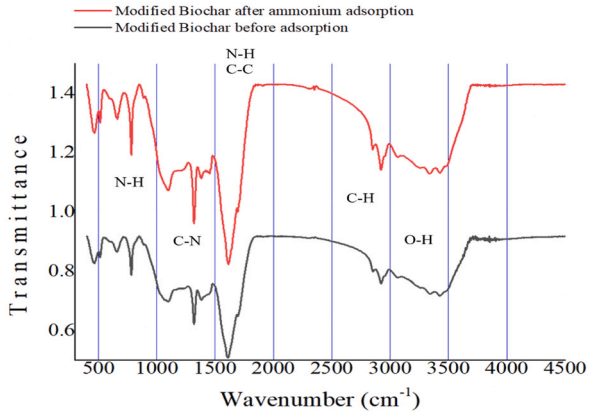

Fig. 3. FT-IR spectrum of the modified biochar.

Table 1
Functional groups in alkali-modified banana-derived biochar.

Wavenumber (cm^{-1})	Functional groups	References
3434	Hydroxy group, H-bonded OH stretch	[33]
3340	Aliphatic primary amine, NH stretch	[33]
2931	Methyne C–H stretch	[33]
2851	Methylene C–H asym./sym. stretch	[33]
1613	Secondary amine, >N–H bend	[33]
1381	gem-Dimethyl or "iso'' (doublet)	[33]
1319	Primary or secondary, OH in-plane bend	[33]
1093	Alkyl-substituted ether, C–O stretch Cyclic ethers, large rings, C–O stretch	[33]
782	C–H 1,3-Disubstitution (meta)	[33]

et al. who investigated biochar derived from recyclable plane tree leaf waste [35]. The results we obtained also agree with previous studies on the oxidative fast pyrolysis of banana leaves in a fluidized bed reactor at 500 °C for 30 min [36].

3.1.4. Surface charge measurements

Zeta potential measurements are important to determine the surface charge of nanoparticles in a colloidal solution [37]. The results show that the biochar surface is negatively charged in the studied pH range, and the values decrease from −28.7 to −43.6 mV when the pH increases from 3 to 10, respectively (Fig. 4).

The zeta potentials decrease as the pH increases. Due to electrostatic attraction, the negative charge on the biochar surface facilitates the adsorption of positively charged species: the greater the electrostatic attraction, the larger the negative charge. Since the zeta potentials are negative and better deprotonation of biochar was reached at higher pH levels, the values we obtained were advantageous for the adsorption of NH_4^+. Similar results have been reported by Huang et al., who determined the zeta potential as a function of pH in a solution containing biochar prepared from cassava residue at 450 °C for 4 h. The zeta potentials they obtained decreased from −15 mV at pH 3 to −33 mV at pH 8 [38]. Deprotonation of C–O functional groups is possible thanks to the alkaline modification, increasing the pH and, as a consequence, resulting in higher NH_4^+ adsorption [39].

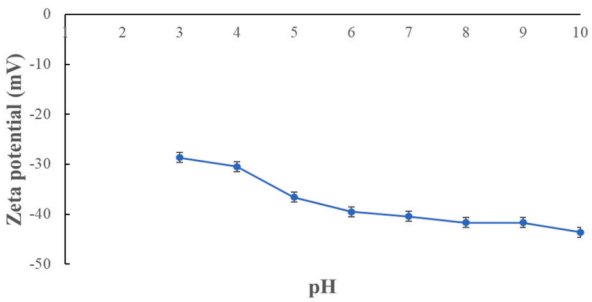

Fig. 4. Zeta potential of biochar as a function of pH (NaCl concentration was 0.01 M).

3.1.5. SSA measurements

The SSA of banana-derived biochar was estimated using the methylene blue method. The experiments were performed three times. The q_{MB} obtained was 0.02173 (mmol/g) and the SSA was 17.01 m^2/g. These results are comparable with the work of Liu et al., where the biochar produced from banana stems and leaves pyrolyzed under 400 °C for 3 h had a SSA of 15.73 m^2/g [2].

In the present study, the SSA was also measured based on the BET adsorption–desorption method. Using this approach, we obtained much smaller SSA values than the previous ones. Several pieces of research on the characterization of biochar showed conclusive results in which the SSA increases with increasing pyrolysis temperature. For most samples, during the repeated measurements, pretreatment for 24 h did not cause a significant difference in the results obtained. The BET SSA for the alkali-modified banana-derived biochar produced in this study was 1.979 m^2/g. This result is similar to the one obtained in the research of Yang et al., who investigated a manganese oxide-modified biochar composite [40]. There difference between the results obtained via these methods is very low. Both methods have limitations: the BET isotherm is recommended by EBC and IBI, but assumes monolayer coverage, while, as demonstrated in the present study, alkali-modified banana-derived biochar follows multilayer adsorption patterns. In any case, many biochar studies indicate that SSA is considered an important characteristic for adsorption, which may be improved by increasing the pyrolysis temperature (an aspect worthy of investigation in the future). The Type II isotherm corresponds to mono–multilayer adsorption according to the IUPAC classification; this isotherm most frequently relates to adsorption occurring for non-porous or macroporous adsorbents with unlimited monolayer–multilayer adsorptions.

The total pore volume obtained was 0.00734 cm^3/g while the average pore diameter was 14.8446 nm. These results indicate that our biochar sample is made up of mesopores according to the IUPAC classification (i.e.: micropores (<2 nm), mesopores (2–50 nm), and macropores (>50 nm)). Fig. 5a) shows the pore diameter distribution and 5b) the adsorption-desorption curves for alkali modified banana derived biochar.

Considering the adsorption capacity (q_e) of our biochar in relation to the SSA for NH_4^+ removal, the q_{max} in the monolayer phase was 0.97 mg/g according to the Langmuir model and the SSA was 1.979 m^2/g according to the BET method. It was calculated that 0.49 mg of NH_4^+ was adsorbed per m^2 surface area on our biochar. Table 2 compares some similar data for different kinds of biochar.

3.2. Ammonium adsorption results

3.2.1. Effect of pH and biochar dose

The adsorption of NH_4^+ is significantly influenced by the pH of the aqueous solution. At lower values of pH (<5), proton H^+ and other cations compete with NH_4^+ for adsorption sites, on the other hand at higher pH values NH_4^+/NH_3 balance shifts towards the production of electrically neutral NH_3 [44]. The effect of pH was investigated in the pH 3–9 range at constant biochar dose and temperature to avoid undesirable and unpredictable pH effects.

The maximum removal rate was 0,4 mg/g, which was obtained using the minimum dose of biochar (200 mg) at room temperature and pH 9 in the presence of only NH_4^+ and biochar at same conditions of temperature and biochar dose The maximum NH_4^+removal percentage of achieved was 25.45 % at pH 9.

Another series of experiments were carried out in order to determine the efficient dose of biochar capable of removing a greater amount of ammonium from the aqueous solution. In these experiments, the pH and temperature values were kept constant (pH 9 and room temperature), while the initial NH_4^+ concentration was 1.5 mg/L. Results showed that the amount of adsorbed NH_4^+ increased with increasing biochar dose and that 0.34 mg/L of NH_4^+ was removed using 500 mg of biochar. Fig. 6 shows the results of analysis of conditions that affected biochar adsorption 6a) effect of pH solution, 6b) NH_4^+ removal percentage, 6c) effect of biochar dose and 6d) the effect of contact time in the adsorption process.

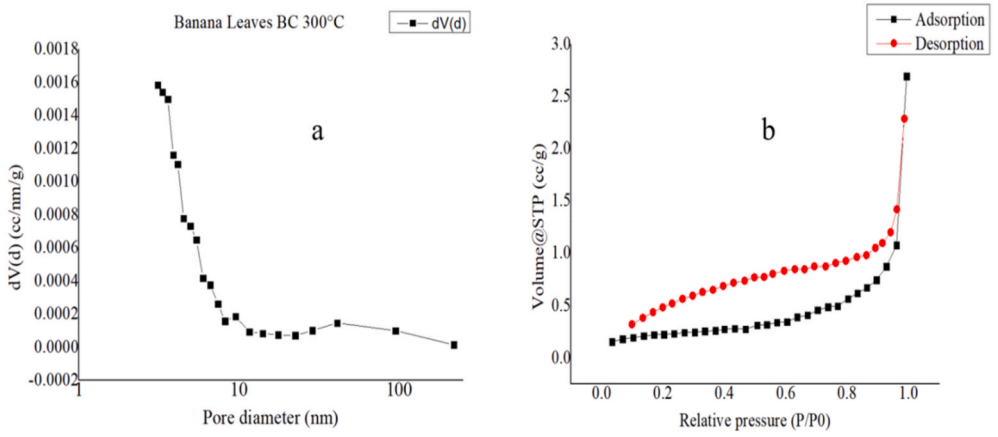

Fig. 5. a) Pore diameter and b) adsorption–desorption curves for alkali-modified banana-derived biochar.

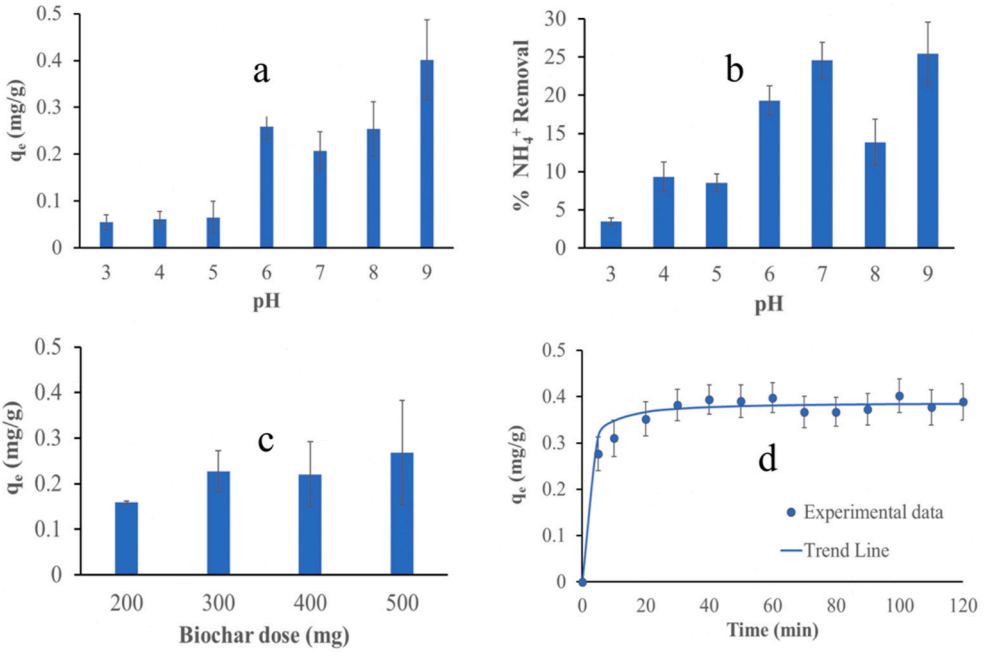

Fig. 6. a) Effect of pH for NH_4^+ removal in aqueous solution with 1.5 mg NH_4^+/L initial concentration and 200 mg of biochar. b) Ammonium removal efficiency based on pH, with 1.5 mg NH_4^+/L initial concentration and 200 mg of biochar. c) Effect of biochar dose on NH_4^+ removal in an aqueous solution containing an initial NH_4^+ concentration of 1.5 mg NH_4^+/L, at pH 9 and room temperature. d) Effect of the contact time in the NH4+ ion removal in an aqueous solution containing an initial NH_4^+ concentration of 1.5 mg NH_4^+/L, at pH 9 and room temperature and 500 mg of biochar.

Table 2
Comparison of q_e and SSA values for ammonium removal using biochar prepared by pyrolysis at 300 °C.

Biochar feedstock	Biochar manufactured conditions	NH_4^+ c_i (mg/L)	q_{max} NH_4^+ mg/g	SSA m^2/g determined by BET isotherm	mgNH_4^+/m^2	References
Rice straw	Biochar pyrolyzed at 300 °C for 2 h under N_2 atmosphere	320	4.090	5.896	0.694	[18]
Phragmites Communis	Biochar pyrolyzed at 300 °C for 2 h under N_2 atmosphere	320	3.206	3.512	0.913	[18]
Sawdust	Biochar pyrolyzed at 300 °C for 2 h under N_2 atmosphere	320	2.201	2.032	1.083	[18]
Orange peel	Biochar pyrolyzed at 300 °C for 2 h	100	4.71	0.55	8.564	[41]
Pineapple peel	Biochar pyrolyzed at 300 °C for 2 h	100	5.60	0.54	10.370	[41]
Raw sesame straw	Biochar pyrolyzed at 300 °C for 2 h under N_2 atmosphere	500	26.84	2.92	9.192	[42]
Fruit pericarp	Biochar pyrolyzed at 300 °C for 2 h under N_2 atmosphere	150	3.25	1.657	1.961	[43]
Banana leaves	NaOH modified biochar pyrolyzed at 300 °C for 2 h	60	5.15	1.979	2.602	This study

3.2.2. Adsorption isotherms

Langmuir and Freundlich isotherm models were considered to investigate monolayer adsorption and calculate the maximum adsorption capacity. Moreover, BET, Harkins–Jura, and AD isotherm models were applied to fit the experimental data obtained for various NH_4^+ concentrations. The following parameters were used: 3.5, 10, 20, 30, 40, and 60 mg NH_4^+/L initial NH_4^+ concentrations, 500 mg biochar dose, room temperature, 250 rpm, and 2 h. The results show that between the Langmuir and Freundlich models, Langmuir fits better the experimental data if only the monolayer phase of the ammonium adsorption is considered, in the context of adsorption of ammonium, it suggests that the adsorption process follows a monolayer adsorption onto a homogeneous surface with no interactions between the adsorbed molecules [45]. On the other hand, the Harkins-Jura isotherm fits the obtained experimental adsorption data the best (Fig. 7). Table 3 summarizes the parameters obtained for the isotherm models, considering the R^2 and χ^2 values of the monolayer adsorption models, Langmuir fits better the experimental data in the interaction of biochar and ammonium (without organic compounds) and the high R^2 in multilayer adsorption process correspond to Harkins-Jura model. Fig. 7 shows the isotherms models applied 7a) monolayer adsorption and 7b) multilayer adsorption.

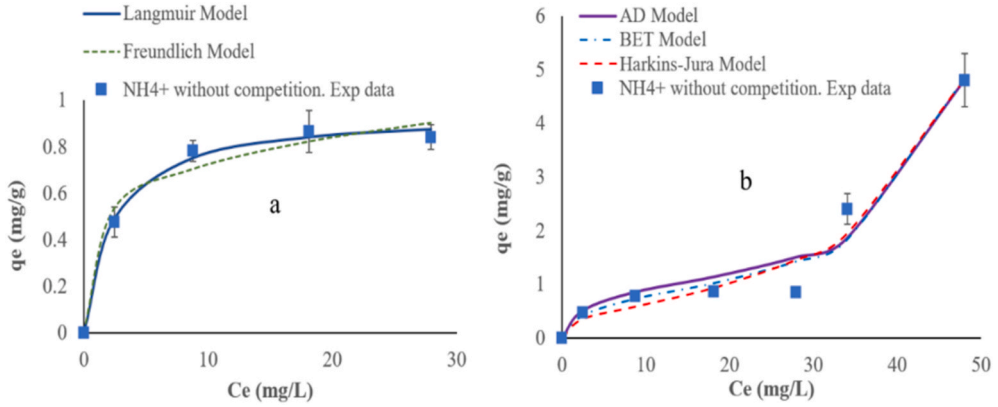

Fig. 7. Isotherm models applied to data obtained for NH_4^+ containing aqueous solution with 500 mg of biochar and different initial NH_4^+ concentrations at pH 9 in 2 h a) monolayer adsorption models and b) multilayer adsorption models.

Table 3
Parameters of isotherm models for NH_4^+ adsorption with banana-derived biochar.

Isotherm Model	Parameters	R^2	χ^2
Langmuir	$K = 0.43984$		
	$q_{max} = 0.947$	0.970	0.001
	$R_L = 0.102$		
Freundlich	$K_f = 0.458$		
	$1/n = 0.20319$	0.841	0.005
BET	$q_m = 0.754$		
	$K_l = 0.0176$	0.950	0.042
	$K_s = 0.428$		
Harkins–Jura	$A = 0.977$	0.954	0.063
	$B = 1.783$		
Aranovich–Donohue	$b_2 = 0.0187$	0.941	0.076
	$n_2 = 0.737$		

After plotting the experimental data, the multilayer isotherm models have an inflection point near the completion of the first adsorbed monolayer. The value of RL is recognized as the dimensionless constant separation factor or equilibrium, which indicates the shape and type of the isotherm that can be either irreversible (RL = 0), favourable (0 < RL < 1), linear (RL = 1), or unfavourable (RL > 1). We obtained an RL value of 0.102, which means that the process is favourable [46].

3.3. Ammonium adsorption in the presence of organic compounds

First, the effect of various organic compounds on NH_4^+ adsorption was investigated separately. The results in this section demonstrate that the parameter that influences adsorption the most is the pH (Fig. 8).

In the analysis of the impact of the presence of organic compounds in the adsorption process, the monolayer and multilayer isotherms models were applied. Figs. 9–11 shows the isotherms models for the organic compounds presence 9a) monolayer models for NH_4^+ adsorption in presence of BSA, 9b) multilayer models for NH_4^+ adsorption in presence of BSA; 10a) monolayer models for NH_4^+ adsorption in presence of lactose, 10b) multilayer models for NH_4^+ adsorption in presence of lactose; 11a) monolayer models for NH_4^+

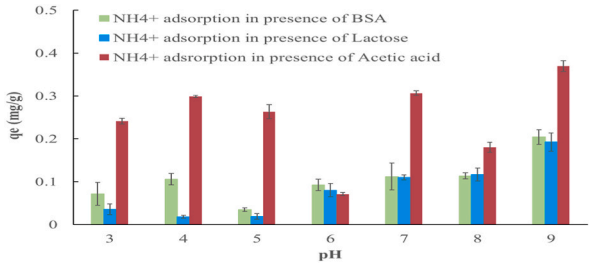

Fig. 8. Effect of pH on NH_4^+ removal in the presence of organic compounds using alkaline-modified banana-derived biochar as an adsorbent. The following initial concentrations were used: 1.5 mg NH_4^+/L, 10 mg/L BSA, 10 mg/L lactose, and 10 mL/L acetic acid.

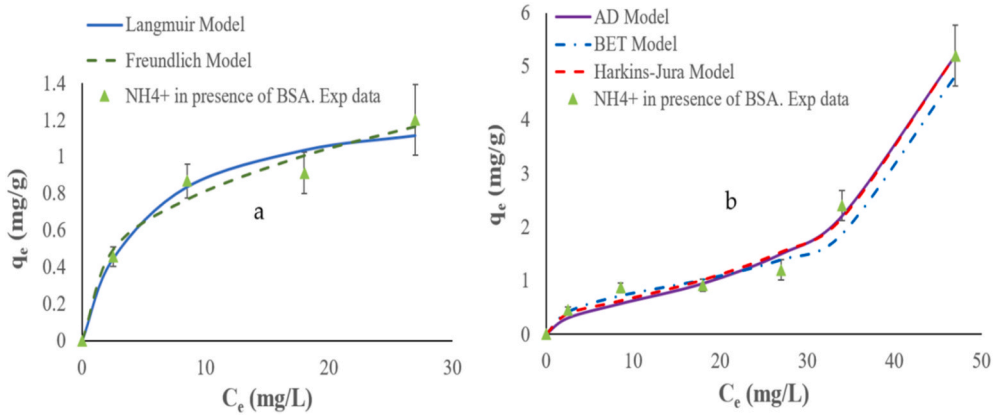

Fig. 9. Isotherm models fitted to data obtained for NH_4^+containing aqueous solution using 500 mg of biochar and different initial NH_4^+ concentrations in the presence of BSA: a) monolayer models, b) multilayer models.

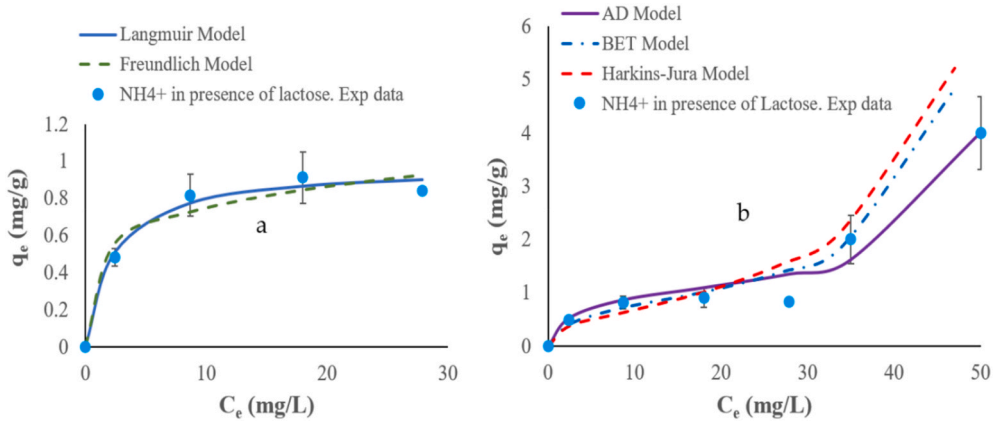

Fig. 10. Isotherm models fitted to data obtained for NH_4^+ containing aqueous solution using 500 mg of biochar and different initial NH_4^+ concentrations in the presence of lactose: a) monolayer models, b) multilayer models.

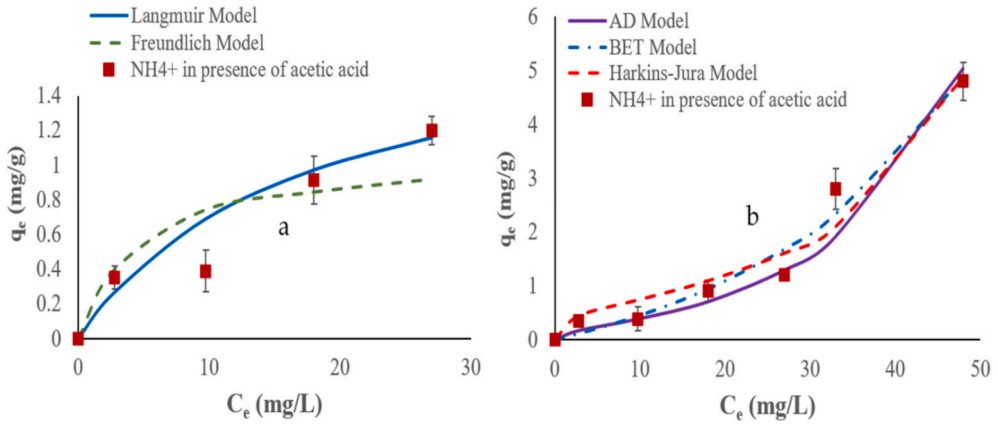

Fig. 11. Isotherm models fitted to data obtained for NH_4^+ containing aqueous solution using 500 mg of biochar and different initial NH_4^+ concentrations in the presence of acetic acid: a) monolayer models, b) multilayer models.

adsorption in presence of acetic acid and 11b) multilayer models for NH_4^+ adsorption in presence of acetic acid.

The Langmuir model in the monolayer phase of NH_4^+ adsorption allows the estimation of the maximum amount of NH_4^+ removed per gram of biochar. In the case of NH_4^+ adsorption in the absence of organic compounds, a value of 0.947 mg/g was reached. This value

increased to 1.132, 0.975, and 1.874 mg/g in the presence of BSA (Fig. 9), lactose (Fig. 10), and acetic acid (Fig. 11), respectively. It is worth to note that the R^2 value of the Langmuir model fitting for acetic acid, for which the highest q_{max} value was obtained, is the lowest of all (0.888). The results have shown that the presence of organic compounds in aqueous solutions can enhance the ammonium adsorption capacities of biochar, situation that can be attributed to increase the cation exchange capacity (CEC) of biochar [16], hydrophobic interactions [47], and modification of biochar surface properties [48]. Fig. 12 shows the possible mechanism of adsorption between the alkali modified biochar derived from banana leaves, ammonium and organic compounds.

Table 4 presents the parameters of isotherms models when ammonium was removed from aqueous solution in presence of organic compounds. In general, for the analysis of NH_4^+ adsorption in the presence of acetic acid, the adjustment factors of the monolayer models are the lowest (Fig. 11). Regarding monolayer phase modelling, Langmuir model fits best in ammonium adsorption in presence of lactose, while in case of the presence of BSA, Freundlich model fits best to the experimental data, taking into account the monolayer phase for small c_e region.

On the other hand, considering the R^2 and χ^2 values of the multilayer adsorption models, in absence of organic compounds, the Harkins-Jura model fits the best, while in presence of BSA, the AD model and Harkins–Jura model give similar fitting. At higher c_e regions, the Harkins-Jura model fits the data the best for lactose, while the BET model fits the data the best for acetic acid.

3.3.1. *Competitive adsorption models*

In the present study, the competitive adsorption was analyzed between biochar, NH_4^+, BSA, lactose, and acetic acid. To apply the AD model derived from Langmuir-like models for the monolayer part of competitive adsorption, we have to analyze the biochar adsorption of each of the aforementioned organic compounds. The concentrations of BSA, lactose, and acetic acid were determined as a function of TOC present in each solution. The initial concentrations of BSA, lactose and acetic acid were 10, 30, and 50 ppm, respectively. The experiments were repeated three times. Table 5 summarizes the parameters obtained in the AD competitive model application. Figs. 13–15 show the curve of AD competitive model between NH_4^+ and organic compounds, 13a) AD competitive model with different initial NH_4^+ concentration in presence of BSA, 13b) AD competitive model with different initial BSA concentrations in presence of NH_4^+; Fig. 14a) AD competitive model with different initial NH_4^+ concentration in presence of lactose, 14b) AD competitive model with different initial lactose concentrations in presence of NH_4^+; Fig. 15a) AD competitive model with different initial NH_4^+ concentration in presence of acetic acid and 15b) AD competitive model with different initial acetic acid concentrations in presence of NH_4^+.

Regarding the results obtained in the adsorption experiments, and despite the small SSAs, the biochar proved to have an excellent adsorption capacity. Both in the presence and absence of organic components, high NH_4^+ removals were obtained. Among the various isotherm models, the Harkins–Jura model gave the best fitting, which demonstrates that NH_4^+ adsorption on alkali-modified banana-derived biochar follows multilayer patterns. The Harkins–Jura isotherm model was analyzed in the work of Ji et al. as well, in which methylene blue was removed using biochar derived from fallen leaves by slow pyrolysis [49].

Finally, this study shows that the NH_4^+ adsorption mechanisms in the presence or absence of organic compounds (BSA, lactose and acetic acid) are different. Ammonium ions were adsorbed due to electrostatic attraction between them and the negatively charged alkaline-modified biochar [41]. However, the adsorption mechanism of ammonium and organic compounds should be different due to their chemical nature; e.g. in case of BSA protein, it contains both positively charged amino and negatively charged acid groups [50], while acetic acid forms negatively charged acetate ions. Pore filling, and electron donor and acceptor (EDA) interaction could be how organic components adsorb onto biochar [51]. The transition from monolayer to multilayer adsorption behaviour at different NH_4^+

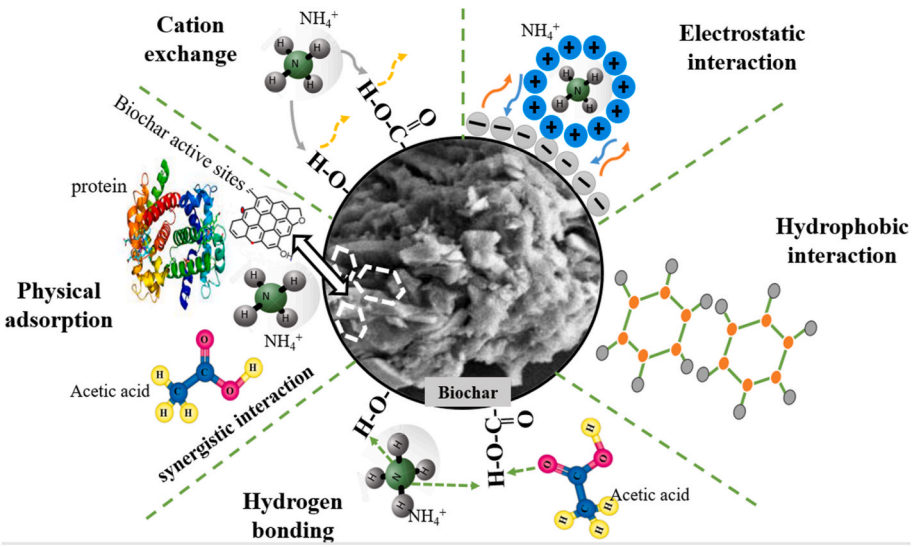

Fig. 12. The possible mechanisms of interactions between alkali modified biochar derived from banana leaves, ammonium and organic compounds (proteins and acids).

Table 4
Parameters of isotherms models for NH_4^+ adsorption using banana-derived biochar in the presence of organic compounds.

Organic Compound	Isotherm Model	Parameters	R^2	χ^2
BSA	Langmuir	$K = 0.204$ $q_{max} = 1.132$ $RL = 0.195$	0.917	0.007
	Freundlich	$K_f = 0.356$ $1/n = 0.3596$	0.924	0.006
	BET	$q_m = 0.745$ $K_l = 0.018$ $K_s = 0.433$	0.956	0.060
	Harkins–Jura	$A = 1.049$ $B = 1.773$	0.985	0.022
	Aranovich–Donohue	$b_2 = 0.011$ $n_2 = 3.159$	0.985	0.022
Lactose	Langmuir	$K = 0.4495$ $q_{max} = 0.975$ $RL = 0.1$	0.933	0.003
	Freundlich	$K_f = 0.463$ $1/n = 0.208$	0.825	0.008
	BET	$q_m = 0.787$ $K_l = 0.017$ $K_s = 0.371$	0.952	0.068
	Harkins–Jura	$A = 0.989$ $B = 1.823$	0.960	0.041
	Aranovich–Donohue	$b_2 = 0.0188$ $n_2 = 0.514$	0.950	0.046
Acetic acid	Langmuir	$K = 0.0596$ $q_{max} = 1.874$ $RL = 0.456$	0.888	0.015
	Freundlich	$K_f = 0.309$ $1/n = 0.251$	0.675	0.045
	BET	$q_m = 20.05$ $K_l = 0.0089$ $K_s = 0.0019$	0.966	0.050
	Harkins–Jura	$A = 1.198$ $B = 1.804$	0.947	0.076
	Aranovich–Donohue	$b_2 = 0.00033$ $n_2 = 186.72$	0.955	0.000

Table 5
Parameters of the AD model for competitive NH_4^+ adsorption using banana-derived biochar in the presence of various organic compounds.

Organic Compound	Parameters	R^2	χ^2
BSA	$b = 0.021$ $n = 0.59$	0.910	0.0899
Lactose	$b = 0.017$ $n = 0.83$	0.902	0.113
Acetic acid	$b = 0.021$ $n = 0.52$	0.947	0.069

concentrations is a consequence of the ion competition for adsorption on the surface of the adsorbent. The experimental data fitted with Type II isotherms means that there is no saturation point when forming a multilayer of ammonium molecules [52].

The adsorption mechanism of the alkaline modified biochar derived from banana leaves can be explained by considering the structure of the adsorbates and the surface characteristics of the adsorbents. Ammonium ion has a positive electric charge and the biochar is been negatively charged facilitates the adsorption. According the elemental composition, biochar had Oxygen, Carbon, Nitrogen, Magnesium, Calcium and Silicon, these components formed important functional groups on the biochar surface, and it becomes effective adsorbent for application in ammonium removal process.

Additionally, the adsorption mechanism of ammonium removal using alkali modified biochar derived from banana leaves in the presence of organic compounds involves considering the interactions between organic compounds and biochar.

4. Conclusions

The interest in biochar is considerable because it is a low-cost, environmentally friendly material capable of contributing to the

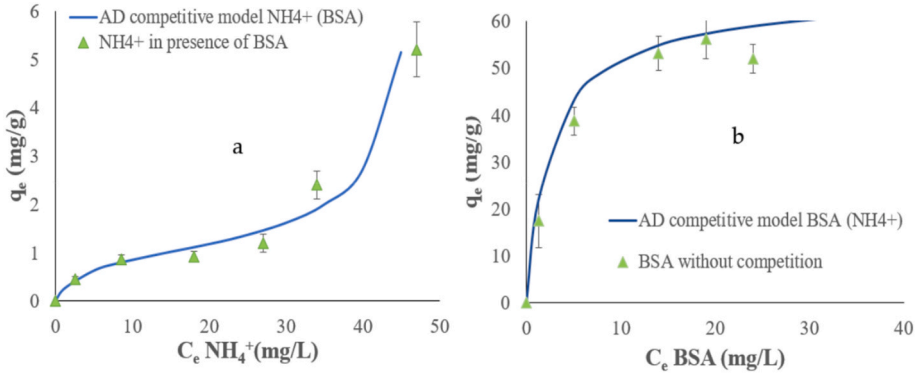

Fig. 13. AD competitive model applied to NH_4^+ containing aqueous solution in the presence of BSA using 200 mg biochar and a) different initial NH_4^+ concentrations and b) different initial BSA concentrations.

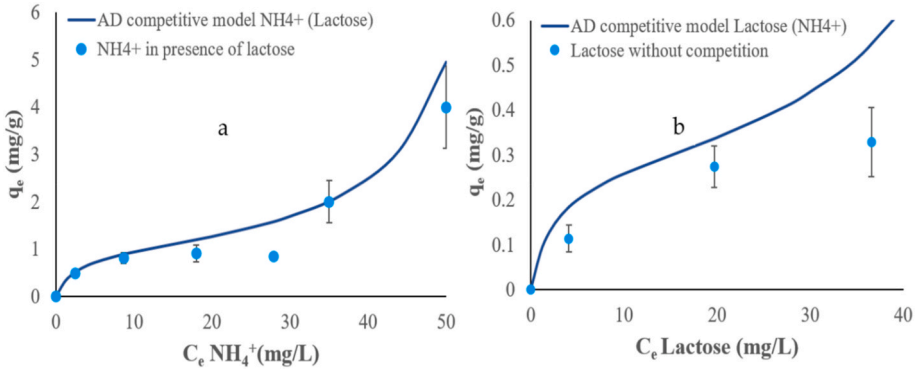

Fig. 14. AD competitive model applied to NH_4^+ containing aqueous solution in the presence of lactose using 200 mg biochar and a) different initial NH_4^+ concentrations and b) different initial lactose concentrations.

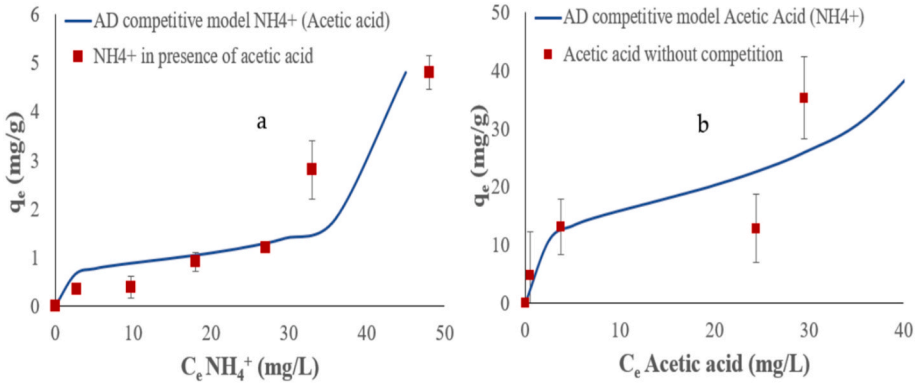

Fig. 15. AD competitive model applied to NH_4^+ containing aqueous solution in the presence of acetic acid using 200 mg biochar and a) different initial NH_4^+ concentrations and b) different initial acetic acid concentrations.

improvement of water quality when used as an adsorbent. In the present work, the impact of various organic compounds on NH_4^+ adsorption was analyzed, demonstrating that the adsorption capacity increases if Langmuir model in monolayer phase is considering, especially in the presence of acids.

The elemental composition of alkali modified biochar derived from banana leaves indicated the presence of Nitrogen, however other properties of the material made it a good ammonium ion adsorbent such as the negative charge surface, cation exchange capacity, the functional groups and the pore size, the presence of organic compounds involves synergistic interactions, achieving in greater ammonium adsorption.

The results obtained demonstrated that the banana-derived biochar is capable of removing NH_4^+ from aqueous solutions; however, the removal percentage does not exceed 30 %. In the monolayer adsorption phase Langmuir isotherm model fits better with the experimental data, in the context of adsorption of ammonium, it suggests that the adsorption process follows a monolayer adsorption onto a homogeneous surface with no interactions between the adsorbed molecules, on the other hand, the high R^2 in multilayer adsorption process correspond to Harkins-Jura model. Therefore, it is necessary to investigate biochar modification technologies further to improve its adsorption capacity while maintaining low production costs.

Until now, there are certainly not enough references for modelling adsorption behaviours in multilayer systems with the presence of organic compounds. The present research offers a novel approach for using a biochar made with an unconventional feedstock of which there are not many studies on its characterization and adsorption capacities, on the other hand the application of ion competition models with models that analyze multilayer adsorption behaviour through the application of the Aranovich-Donohue equation derived from the Langmuir-like model.

Moreover, the present work leaves a precedent of how to convert an agricultural waste material into an adsorbent for a eutrophicating compound such as ammonium from wastewater. Evidently, the replication and large-scale application of the use of biochar produced through banana leaves will contribute to giving a useful life to the large amount of agricultural waste in countries where bananas are massively cultivated, promoting the concept of circular economy and can additionally remove pollutants from wastewater to be returned to the environment in better quality. In the future, studies are necessary on both the simultaneous adsorption or co-adsorption of ammonium and phosphates using biochar derived from banana leaves and the recovery of biochar containing ammonium and the closure of its cycle using it as a soil fertilizer.

Funding statement

The University of Szeged supported Open Access Funding (grant number: 6760).

Data availability statement

Data included in article/supp. material/referenced in article.

CRediT authorship contribution statement

Fernanda Pantoja: Writing – original draft, Investigation. **Sándor Beszédes:** Writing – review & editing, Supervision. **Tamás Gyulavári:** Writing – review & editing, Validation. **Erzsébet Illés:** Validation. **Gábor Kozma:** Validation. **Zsuzsanna László:** Writing – review & editing, Supervision.

Declaration of competing interest

The authors declare that they have no known competing financial interests or personal relationships that could have appeared to influence the work reported in this paper.

Acknowledgments

Project no. 2019-2.1.11-TÉT-2020-00152 has been implemented with the support provided by the Ministry of Innovation and Technology of Hungary.

References

[1] UN, The 2030 Agenda and the Sustainable Development Goals an Opportunity for Latin America and the Caribbean, 2018 [Online]. Available: https://repositorio.cepal.org/bitstream/handle/11362/40156/25/S1801140_en.pdf.
[2] X. Liu, G. Li, C. Chen, X. Zhang, K. Zhou, X. Long, Banana stem and leaf biochar as an effective adsorbent for cadmium and lead in aqueous solution, Sci. Rep. 12 (1) (2022) 1–14, https://doi.org/10.1038/s41598-022-05652-7.
[3] E. Rosa, H. Arriaga, P. Merino, Strategies to mitigate ammonia and nitrous oxide losses across the manure management chain for intensive laying hen farms, Sci. Total Environ. 803 (2022) 150017, https://doi.org/10.1016/j.scitotenv.2021.150017.
[4] X. Li, C. Wang, J. Zhang, J. Liu, B. Liu, G. Chen, Preparation and application of magnetic biochar in water treatment: a critical review, Sci. Total Environ. 711 (2020) 134847, https://doi.org/10.1016/j.scitotenv.2019.134847.
[5] F. Obi, B. Ugwuishiwu, J. Nwakaire, Agricultural waste concept, generation, utilization and management, Niger. J. Technol. 35 (4) (2016) 957, https://doi.org/10.4314/njt.v35i4.34.
[6] FAO, Market Review Preliminary Results 2022, 2022.
[7] C. Wang, et al., Biochar-based slow-release of fertilizers for sustainable agriculture: a mini review, Environ. Sci. Ecotechnology 10 (2022) 100167, https://doi.org/10.1016/j.ese.2022.100167.
[8] P. Alexander, A. Arneth, R. Henry, J. Maire, S. Rabin, M.D.A. Rounsevell, High energy and fertilizer prices are more damaging than food export curtailment from Ukraine and Russia for food prices , health and the environment 4 (January) (2022), https://doi.org/10.1038/s43016-022-00659-9.
[9] X. Cai, L. Yao, Y. Hu, R.A. Dahlgren, Effects of aquatic nitrogen pollution on particle-attached ammonia-oxidizing bacteria in urban freshwater mesocosms, World J. Microbiol. Biotechnol. 38 (4) (2022) 1–12, https://doi.org/10.1007/s11274-022-03251-2.
[10] A. Krishan, A. Srivastava, Recovery of nutrients from dairy wastewater by struvite crystallization, Int. J. Eng. Res. Gen. Sci. 3 (5) (2015) 591–597 [Online]. Available: https://citeseerx.ist.psu.edu/document?repid=rep1&type=pdf&doi=c91ee465f7fca622bfa598ebe068effa681c8741.
[11] J. Huang, N.R. Kankanamge, C. Chow, D.T. Welsh, T. Li, P.R. Teasdale, Removing ammonium from water and wastewater using cost-effective adsorbents: a review, J. Environ. Sci. (China) 63 (2018) 174–197, https://doi.org/10.1016/j.jes.2017.09.009.

[12] Q. Yin, R. Wang, Z. Zhao, Application of Mg–Al-modified biochar for simultaneous removal of ammonium, nitrate, and phosphate from eutrophic water, J. Clean. Prod. 176 (2018) 230–240, https://doi.org/10.1016/j.jclepro.2017.12.117.

[13] T.M. Vu, et al., Removing ammonium from water using modified corncob-biochar, Sci. Total Environ. 579 (2017) 612–619, https://doi.org/10.1016/j.scitotenv.2016.11.050.

[14] R. Li, et al., Simultaneous capture removal of phosphate, ammonium and organic substances by MgO impregnated biochar and its potential use in swine wastewater treatment, J. Clean. Prod. 147 (2017) 96–107, https://doi.org/10.1016/j.jclepro.2017.01.069.

[15] Y. Qin, et al., Enhanced removal of ammonium from water by ball-milled biochar, Environ. Geochem. Health 42 (6) (2020) 1579–1587, https://doi.org/10.1007/s10653-019-00474-5.

[16] X. Gai, H. Wang, J. Liu, L. Zhai, S. Liu, T. Ren, "Effects of Feedstock and Pyrolysis Temperature on Biochar Adsorption of Ammonium and Nitrate," (3) (2014) 1–19, https://doi.org/10.1371/journal.pone.0113888.

[17] W. Zheng, M. Guo, T. Chow, D.N. Bennett, N. Rajagopalan, Sorption properties of greenwaste biochar for two triazine pesticides, J. Hazard Mater. 181 (1–3) (2010) 121–126, https://doi.org/10.1016/j.jhazmat.2010.04.103.

[18] D. Xu, J. Cao, Y. Li, A. Howard, K. Yu, Effect of pyrolysis temperature on characteristics of biochars derived from different feedstocks: a case study on ammonium adsorption capacity, Waste Manag. 87 (2019) 652–660, https://doi.org/10.1016/j.wasman.2019.02.049.

[19] N. Vu, K. Do, Insights into Adsorption of Ammonium by Biochar Derived from Low Temperature Pyrolysis of Coffee Husk, 2023, pp. 2193–2205.

[20] H. Sukmana, et al., Hungarian and Indonesian rice husk as bioadsorbents for binary biosorption of cationic dyes from aqueous solutions: a factorial design analysis, Heliyon 9 (6) (2023) e17154, https://doi.org/10.1016/j.heliyon.2023.e17154.

[21] J.H. Park, et al., Competitive adsorption of heavy metals onto sesame straw biochar in aqueous solutions, Chemosphere 142 (2016) 77–83, https://doi.org/10.1016/j.chemosphere.2015.05.093.

[22] C.A. Nunes, M.C. Guerreiro, Estimation of surface area and pore volume of activated carbons by methylene blue and iodine numbers, Quim. Nova 34 (3) (2011) 472–476, https://doi.org/10.1590/S0100-40422011000300020.

[23] A. Albalasmeh, et al., Characterization and Artificial Neural Networks Modelling of methylene blue adsorption of biochar derived from agricultural residues: effect of biomass type, pyrolysis temperature, particle size, J. Saudi Chem. Soc. 24 (11) (2020) 811–823, https://doi.org/10.1016/j.jscs.2020.07.005.

[24] A. Hossain, H.H. Ngo, W. Guo, Introductory of Microsoft Excel SOLVER function - spreadsheet method for isotherm and kinetics modelling of metals biosorption in water and wastewater 3 (4) (2013) 223–237.

[25] B. Abebe, H.C.A. Murthy, E. Amare, Summary on adsorption and photocatalysis for pollutant remediation: mini review, J. Encapsulation Adsorpt. Sci. 8 (4) (2018) 225–255, https://doi.org/10.4236/jeas.2018.84012.

[26] K.A. Alkhamis, D.E. Wurster, Prediction of adsorption from multicomponent solutions by activated carbon using single-solute parameters. Part II - proposed equation, AAPS PharmSciTech 3 (3) (2002), https://doi.org/10.1007/BF02830621.

[27] G. de V. Brião, M.G.C. da Silva, M.G.A. Vieira, K.H. Chu, Correlation of type II adsorption isotherms of water contaminants using modified BET equations, Colloids Interface Sci. Commun. 46 (2022), https://doi.org/10.1016/j.colcom.2021.100557.

[28] Y. Cao, L. Wang, X. Kang, J. Song, H. Guo, Q. Zhang, Insight into atrazine removal by fallen leaf biochar prepared at different pyrolysis temperatures: batch experiments, column adsorption and DFT calculations, Environ. Pollut. 317 (September 2022) (2023) 120832, https://doi.org/10.1016/j.envpol.2022.120832.

[29] M.I. Rafique, A.R.A. Usman, M. Ahmad, A. Sallam, M.I. Al-Wabel, In situ immobilization of Cr and its availability to maize plants in tannery waste–contaminated soil: effects of biochar feedstock and pyrolysis temperature, J. Soils Sediments 20 (1) (2020) 330–339, https://doi.org/10.1007/s11368-019-02399-z.

[30] T. Ali, et al., Contrasting effects of banana peels waste and its biochar on greenhouse gas emissions and soil biochemical properties, Process Saf. Environ. Protect. 122 (2019) 366–377, https://doi.org/10.1016/j.psep.2018.10.030.

[31] Ć.-P.I. Bednik M, A. Medyńska-Juraszek, Effect of six different feedstocks on biochar ' s properties and expected stability, Agronomy 12 (7) (2022), https://doi.org/10.3390/agronomy12071525.

[32] Q. Min, L. Riaz, A. Ali, Employment of Cannabis sativa biochar to improve soil nutrient pool and metal immobilization, Front. Environ. Sci. (October) (2022) 1–16, https://doi.org/10.3389/fenvs.2022.1011820.

[33] A.B.D. Nandiyanto, R. Oktiani, R. Ragadhita, How to read and interpret ftir spectroscope of organic material, Indones. J. Sci. Technol. 4 (1) (2019) 97–118, https://doi.org/10.17509/ijost.v4i1.15806.

[34] M. Tan, Y. Li, D. Chi, Q. Wu, Efficient removal of ammonium in aqueous solution by ultrasonic magnesium-modified biochar 461 (January) (2023), https://doi.org/10.1016/j.cej.2023.142072.

[35] X. Yang, et al., Sorptive removal of ibuprofen from water by natural porous biochar derived from recyclable plane tree leaf waste, J. Water Process Eng. 46 (February) (2022) 102627, https://doi.org/10.1016/j.jwpe.2022.102627.

[36] N. Sellin, D.R. Krohl, C. Marangoni, O. Souza, Oxidative fast pyrolysis of banana leaves in fluidized bed reactor, Renew. Energy 96 (2016) 56–64, https://doi.org/10.1016/j.renene.2016.04.032.

[37] A. Kumar, C.K. Dixit, Methods for characterization of nanoparticles, Adv. Nanomedicine Deliv. Ther. Nucleic Acids (2017) 44–58, https://doi.org/10.1016/B978-0-08-100557-6.00003-1.

[38] P. Huang, et al., Effects of metal ions and pH on ofloxacin sorption to cassava residue-derived biochar, Sci. Total Environ. 616–617 (2018) 1384–1391, https://doi.org/10.1016/j.scitotenv.2017.10.177.

[39] X. Li, X. Jiang, Y. Song, S.X. Chang, Coexistence of polyethylene microplastics and biochar increases ammonium sorption in an aqueous solution, J. Hazard Mater. 405 (August 2020) (2021) 124260, https://doi.org/10.1016/j.jhazmat.2020.124260.

[40] Z. Yu, L. Zhou, Y. Huang, Z. Song, W. Qiu, Effects of a manganese oxide-modified biochar composite on adsorption of arsenic in red soil, J. Environ. Manag. 163 (2015) 155–162, https://doi.org/10.1016/j.jenvman.2015.08.020.

[41] X. Hu, et al., Comparison study on the ammonium adsorption of the biochars derived from different kinds of fruit peel, Sci. Total Environ. 707 (2020) 135544, https://doi.org/10.1016/j.scitotenv.2019.135544.

[42] Q. Yin, B. Zhang, R. Wang, Z. Zhao, Phosphate and ammonium adsorption of sesame straw biochars produced at different pyrolysis temperatures, Environ. Sci. Pollut. Res. 25 (5) (2018) 4320–4329, https://doi.org/10.1007/s11356-017-0778-4.

[43] S. Xue, et al., Food waste based biochars for ammonia nitrogen removal from aqueous solutions, Bioresour. Technol. 292 (June) (2019) 121927, https://doi.org/10.1016/j.biortech.2019.121927.

[44] D. Ngoc, G. Ngo, X. Chuang, C. Huang, L. Hua, Compositional characterization of nine agricultural waste biochars : the relations between alkaline metals and cation exchange capacity with ammonium adsorption capability, J. Environ. Chem. Eng. 11 (3) (2023) 110003, https://doi.org/10.1016/j.jece.2023.110003.

[45] Y. Yao, et al., Removal of phosphate from aqueous solution by biochar derived from anaerobically digested sugar beet tailings, J. Hazard Mater. 190 (1–3) (2011) 501–507, https://doi.org/10.1016/j.jhazmat.2011.03.083.

[46] T. Wang, D. Zhang, K. Fang, W. Zhu, Q. Peng, Z. Xie, Enhanced nitrate removal by physical activation and Mg/Al layered double hydroxide modified biochar derived from wood waste: adsorption characteristics and mechanisms, J. Environ. Chem. Eng. 9 (4) (2021) 105184, https://doi.org/10.1016/j.jece.2021.105184.

[47] M. Inyang, E. Dickenson, The potential role of biochar in the removal of organic and microbial contaminants from potable and reuse water : a review, Chemosphere 134 (2015) 232–240, https://doi.org/10.1016/j.chemosphere.2015.03.072.

[48] D. Hsu, C. Lu, T. Pang, Y. Wang, G. Wang, Adsorption of ammonium nitrogen from aqueous solution on chemically activated biochar prepared from sorghum distillers grain, Appl. Sci. (2019), https://doi.org/10.3390/app9235249.

[49] B. Ji, J. Wang, H. Song, W. Chen, Removal of methylene blue from aqueous solutions using biochar derived from a fallen leaf by slow pyrolysis: behavior and mechanism, J. Environ. Chem. Eng. 7 (3) (2019) 103036, https://doi.org/10.1016/j.jece.2019.103036.

[50] U. Scheler, Effective Charge of Bovine Serum Albumin Determined by Electrophoresis NMR Ute Bo, vol. 435, 2007, pp. 342–345, https://doi.org/10.1016/j.cplett.2006.12.068.
[51] Z. Abbas, et al., A critical review of mechanisms involved in the adsorption of organic and inorganic contaminants through biochar, Arabian J. Geosci. 11 (448) (2018), https://doi.org/10.1007/s12517-018-3790-1.
[52] R. Kecili, C.M. Hussain, Mechanism of Adsorption on Nanomaterials, Elsevier Inc., 2018, https://doi.org/10.1016/B978-0-12-812792-6.00004-2.